Recent Developments in Mixed Ionic and Electronic Conducting Electrodes for the Alkali Metal Thermal Electric Converter (AMTEC)

Robert W. Fletcher[1, 2] and Johannes W. Schwank[2]

[1]*Advanced Modular Power Systems (AMPS), 4370 Varsity Drive, Ann Arbor, Michigan 48108*
[2]*Department of Chemical Engineering, University of Michigan, 2300 Hayward Street, 3030 H.H. Dow Building, Ann Arbor, Michigan 48109-2136*
734-677-4260, ext. 202; fax: 734-677-0704; rfletcher@ampsys.com

Abstract. Mixed ionic and electronic conducting electrodes (MIECEs) have recently gained more attention in the development of the Alkali Metal Thermal Electric Converter (AMTEC). The advantage of MIECEs, as their name implies, is that they allow both electronic transport and ionic transport within the matrix of their materials. This lowers charge transport resistances, which lowers overall electrical resistances of the electrochemical system, and, thus, can improve reaction rates for a given apparent or superficial surface area of the electrode. The AMTEC system is a self-contained, self-regenerating compact technology that electrochemically converts heat directly to electricity. Our latest developments for AMTEC MIECEs are presented. These include electrodes formulated from various blends of titanium nitride or molybdenum with titanium dioxide. The general formulation, application, processing and testing methods for these electrodes are presented. Measured power densities of selected MIECEs are given. The physical morphology, and composition of our MIECEs are also described. Finally, a possible operational mechanism for these electrodes is proposed.

INTRODUCTION AND BACKGROUND

The theoretical operation of the Alkali Metal Thermal Electric Converter (AMTEC) has been extensively discussed in the literature and will not be reviewed here. Because AMTEC systems are power generators, this work focuses on current-carrying electrodes. There are two types of current carrying AMTEC electrodes, electron-carriers only, and electrodes that conduct both electrons and ions. Electron-carrying electrodes transport only electrons to, or from, the surface of the solid electrolyte permitting reduction or oxidation of the transported ionic species. The adsorption or desorption of the neutral forms of the transported ionic species from the gas or liquid phase add additional complexity to the system. These electrochemical events coincide at the three-phase boundary (TPB) interface between the electrolyte, electrode, and gas. In AMTEC systems this TPB involves β"-alumina solid electrolyte (BASE), an electrode (such as sputtered TiN, see Figure 1a below) and sodium (vapor or liquid). Some level of "porosity" of the electrode is necessary to permit diffusion of the neutral species through the electrode, normally along grain boundaries or via actual pores. To be effective, the transport paths must be at least as large as the transported molecules or atoms. If this requirement is not met in the case of AMTEC, then transport of the neutral sodium will be hindered, and this manifests itself as an electrical impedance. Conversely, high electrode porosity may reduce diffusional limitations, but will tends to increase the electrical resistive impedance, and may reduce the numerical density of the TPB sites on the electrolyte interface.

Mixed ionic-electronic conducting electrodes (MIECEs) exhibit both electronic (electron, or hole) and ionic conductivity. Generally, these materials have electronic conductivities lower than metals, and ionic conductivities well below those of the fast ion conductors. In AMTEC systems MIECE materials must have a high enough concentration of disordered defects containing the mobile sodium ions in the lattice, or amorphous, structure that they are able to overcome the binding energies within the structural framework with relative ease. The matrix must also contain either *n*, or *p* type dopants to act as electron donors or acceptors while not impeding ionic conduction. The initial work outlined here indicates that a MIECE for an AMTEC system has been successfully developed. A

CP654, *Space Technology and Applications International Forum–STAIF 2003*, edited by M.S. El-Genk

more detailed review of AMTEC electrode development by these authors and others is documented in previous work. (Fletcher, Schwank, 2002)

EXPERIMENTAL

Only a general description of the process and formulations are provided here because the methods for producing these electrodes are now under consideration for patent protection. A description of various aspects of these activities has been given before (Fletcher, Schwank, 2002). The BASE used in these experiments was tubular with one open end and one closed end (Ionotec, UK). The tubes were approximately 12 cm long, with an outer diameter (OD) of 1.5 cm and wall thickness of 1.0 mm. BASE tubes were suitably dried and prepared prior to electrode application.

Numerous formulations of dry molybdenum powder mixed at different ratios with dry titanium dioxide (anatase) powder, and titanium hydride powder mixed at different ratios with dry titanium dioxide (anatase) powder were sintered to yield various matrixes of Mo/TiO_2 and TiN/TiO_2. Presented here are test data from the titanium nitride/titanium dioxide formulations. The powders were blended as previously described. Various test electrodes, made by manually painting the suspended slurries on the OD of the BASE tubes as thin-coated bands, approximately 1.27 cm long. Electrode surface areas on the BASE were typically 6.0 cm^2, and ranged from 15 to 50 μm thick. For experimental purposes, multiple electrodes, each from a different slurry formulation, were painted on the OD of different BASE tubes for each set of tests. Once applied, the painted electrodes were allowed to air dry and the BASE tube/electrodes were then placed in a high-temperature sintering oven for processing. Several heating ramp rates, different sintering temperatures, heat-soak times, and cooling rate profiles were studied. Heating and cooling ramp rates were, however, limited by the heat transfer capabilities of the sintering furnace.

After sintering, the electrodes were generally found to be durable and well bonded to the surface of the BASE tube. Figure 1b below is a scanning electron micrograph of one of the molybdenum and titanium dioxide blends evaluated. The level of porosity and degree of sintering is uniform throughout the matrix and in the desired range. TiN/TiO_2 formulations looked similar to those of Figure 1a. An additional titanium nitride (TiN) electrode of dimensions similar to the painted electrodes was also sputtered on the OD of the BASE tube. Sputtered TiN electrodes such as that shown in Figure 1b are currently the standard electrodes used in AMTEC systems and serve as excellent controls for comparison with the sintered test electrodes.

With electrodes applied, the BASE tube is assembled into a Miniature Electrode Test Cell (METC). The METC produces electrical power and is an active system. It, however, has no sodium recirculation, so once the sodium reservoir is depleted, the useful life of the device has ended. The benefit of the METC is that it represents the true behavior of an electrode in an actual functional configuration; the device has been described in the literature (Hunt, et al., 1997). Figure 2a below shows a four electrode BASE tube ready for final assembly into an METC. METCs typically have an all stainless-steel housing and contain only one BASE tube assembly. The METC BASE tubes can have one or more electrodes applied allowing simultaneous evaluation. Each electrode is fitted with separate current and voltage leads connected to feedthroughs at the cold end (also known as the condenser end) of the METC. Such multi-electrode configurations significantly improve METC utility, allowing direct in-situ comparisons between various electrodes. Next, the assembly is vacuum-pumped, baked out, and the cell charged with sodium.

Figure 2b illustrates an assembly schematic of an METC with housing walls cut away to expose a BASE tube with two electrodes. The major components of the METC numbered in Figure 2b are defined as follows: 1) electrode #1 cathode feedthrough lead; 2) electrode #2 cathode feedthrough lead; 3) electrode #1 voltage lead; 4) electrode #2 voltage lead; 5) condenser chamber and evaporator chamber pump-out ports and valves; 6) electrode #1; 7) BASE tube assembly; 8) electrode #2; 9) METC housing outer wall; 10) a closed-end metal thermocouple well that runs the internal length of the BASE tube through to the exterior of the cell allowing temperature measurement in the BASE tube; 11) reservoir for the initial sodium load, also called the evaporator or hot end; 12) sodium reservoir thermocouple well.

Once the METC is charged with sodium, it is then made ready for testing with adequately insulated multiple heaters on the cell exterior walls. These are operated with thermocouple reading controllers to allow various test temperature profiles. The assembly is placed in a data acquisition test-bed fitted with a PC type lab computer used for electrode testing. In the experimental work discussed here, liquid sodium is both the anode electrode and its

current collector. Operating in this "liquid-anode" mode allows experimental focus on the performance of the cathode only, and permits direct one-to-one comparisons between various cathode designs.

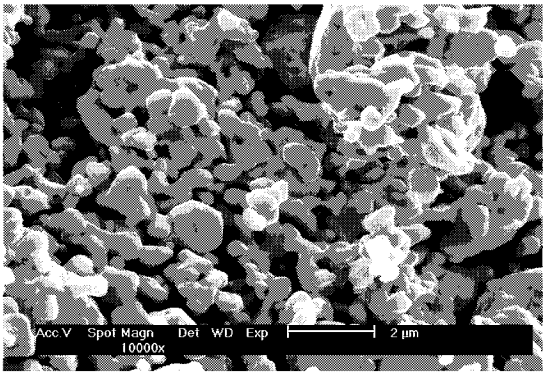

(a) Sintered Metal and TiO_2 Electrode.

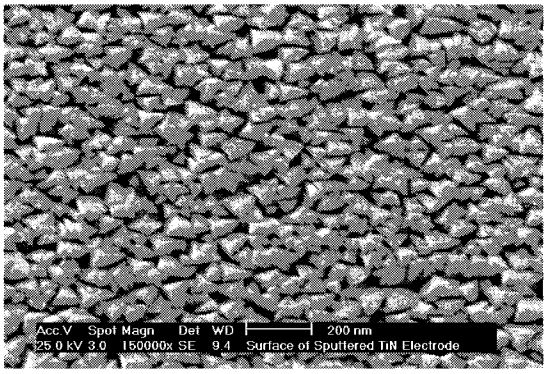

(b) Sputtered Titanium Nitride Electrode.

FIGURE 1. SEM Micrograph of (a) 10,000x's Magnification of a Sintered Metal Mixed Conductor Electrode Currently Under Study for AMTEC Systems, and (b) 150,000x's Magnification of a Sputtered TiN Electrode Typically Used in AMTEC Systems. *(Both photos by R. Fletcher)*

(a) Four Electrode METC BASE Tube.

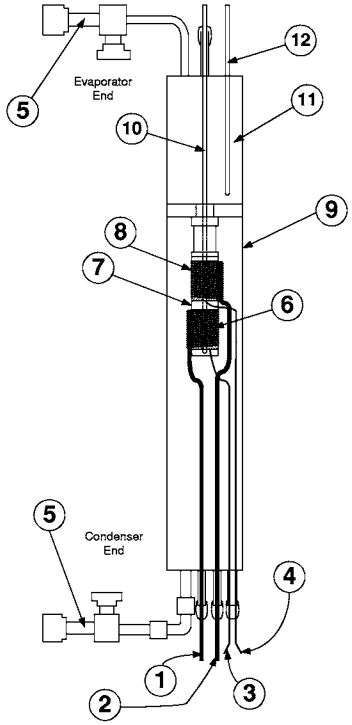

(b) Schematic of a Two-Electrode METC.

FIGURE 2. Illustrations Showing (a) a Four-Electrode BASE Tube with the Related Wire-Wrapped Current Collectors and Electrical Leads Just Before Final Assembly into an METC, and (b) a See-Though Schematic of an METC Assembly with a Two-Electrode BASE Tube. (The various numbered items are described in the text above.)

RESULTS AND DISCUSSION

Current-voltage (I-V) polarization sweeps were generated using the METC test configuration described above. All test data presented here were collected using liquid sodium as the anode and I-V sweep rates of 0.5 amps/second. Figure 3a below shows typical METC test data plots for BASE tube temperatures of 700°C, 750°C, 800°C and 850°C for our standard sputtered TiN cathode electrode. Open circuit voltages (Voc) for these I-V sweeps are around 1.0 volt (the left "Y" axis of the chart) and are a function of BASE temperature and sodium vapor pressure. These data terminate at approximately 1.5 to 1.75 amps/cm^2 due to the limitations of the power supply used in these tests. The complete I-V sweep cycle initiates from zero amps at Voc and continuously sweeps at the designated rate up to the maximum power supply current, and then continuously sweeps back to zero current and Voc. Comparing the forward I-V sweep data to the return I-V sweep data can provide valuable insights into electrode performance.

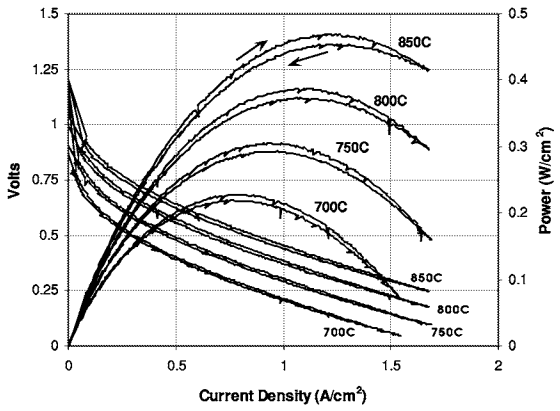

(a) The Standard TiN Electrode.

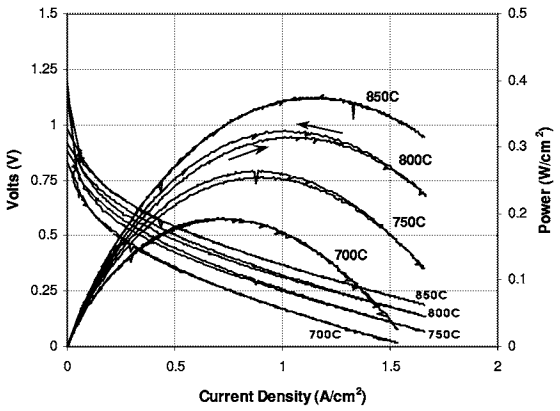

(b) Test Electrode Made From Sintered TiN/TiO_2.

FIGURE 3. Current-Voltage Polarization Sweeps with Power Plots. (These METC test data collected were at 700°C, 750°C, 800°C and 850°C BASE tube temperatures using liquid sodium as the anode. The arrows on the power plot indicate the ascending and the descending sweep values.)

Related power plots calculated in Watts/cm^2 are also displayed and are scaled to the secondary "Y" axis on the right of each chart. In Figure 3a, the power plot for the 850°C data shows two arrows. Similar arrows would apply equally to all the test temperatures but have been omitted for clarity. The arrow pointing to the right indicates the power plot for the ascending I-V sweep starting from Voc and zero amps to the peak current for the power supply. The arrow pointing to the left indicates the returning sweep from the maximum power supply current back to zero amps and Voc. A reduction in power is observed during the return leg of I-V sweeps for each of these BASE tube temperatures. This return sweep power reduction is caused by localized cooling of the electrode and the BASE due to loss of the heat of vaporization of the neutral sodium evaporating from the surface of the cathode reducing the output voltage. Since the sodium ion conductivity of the BASE is a function of temperature this decrease in BASE temperature also reduces the ionic conductivity of the BASE causing a transient increase in ionic resistivity. In addition, during converter operation the transporting sodium ions carry thermal energy across the BASE. Though less significant, the return I-V sweep continuously reduces sodium ion flow with a corresponding reduction in sodium ion thermal energy transported across the BASE. These combined phenomena in the return I-V sweep cause the cooling that results in the power drop observed in Figure 3a. (In stable temperature AMTEC systems at nearly constant current loads such power decreases are not encountered.) This transient cooling can be substantial, depending upon the sweep rate. Liquid sodium in the BASE tube at the electrode typically dropped by 18°C to 24°C at the peak I-V sweep current. Detailed analytical modeling of these transient surface temperature effects is yet to be completed. Peak current densities of 0.45 Watts/cm^2 are typical for sputtered TiN electrodes at 850°C.

Figure 3b above presents comparable I-V sweeps of a test MIECE made from sintered TiN and TiO_2. I-V sweep rates and calculated power plots for the test electrode are illustrated for the same BASE temperatures as those in Figure 3a. They display, however, significantly different characteristics than those from the standard sputtered TiN electrode. The typical loss in return I-V sweep power is not observed for the MIECE even though I-V sweep rates of 0.5 amps/sec (and, therefore, sodium ion transport rates across the BASE) are identical for the two electrodes.

The return I-V sweep and resulting power are comparable or higher than those for the first half of the sweep in Figure 3b. Note the direction and position of the arrows in Figure 3b. Such behavior is not seen in solely electronic conducting AMTEC electrodes. Monitoring of temperatures inside the BASE tube reveals that the sintered TiN/TiO_2 electrode experiences the same thermal drop as the sputtered TiN electrode, and should thus display the same power loss levels as the sputtered TiN electrode on the return sweep. This, however, is not the case. Electrode performance is comparable, or improved on the return sweep and more than compensates for any power losses due to reduced sodium ion thermal transport and sodium evaporative cooling.

The improved electrode performance in the return sweep in Figure 3b is due to two events related to the presence of TiO_2 in the electrode matrix. First, TiO_2 is known to exhibit increased electronic conductivity at elevated temperatures when the partial pressure of oxygen, $p(O_2)$, is reduced (Nowotny, et al., 1998). Sodium is a well-known oxygen scavenger and the increased presence of sodium vapor causes TiO_2 to lose some oxygen in its matrix, increasing TiO_2 electronic conductivity. Second, TiO_2 is known to form various sodium titanate complexes that display high sodium ion conductivity (Bando, et al., 1980; Ryan, et al., 2001). These sodium titanate complexes have also been shown to display significantly increased ionic conductivity in the presence of increasing sodium vapor partial pressures (Ryan, et al., 1999). An interesting aspect of our sintered TiN/TiO_2 electrodes is that they required no sodium vapor conditioning of 48 to 72 hours, as discussed by Ryan (Ryan, et al., 2001). These TiN/TiO_2 electrodes displayed peak operational performance on the first I-V sweep and maintained these capabilities for the useful, though limited, life of the METC.

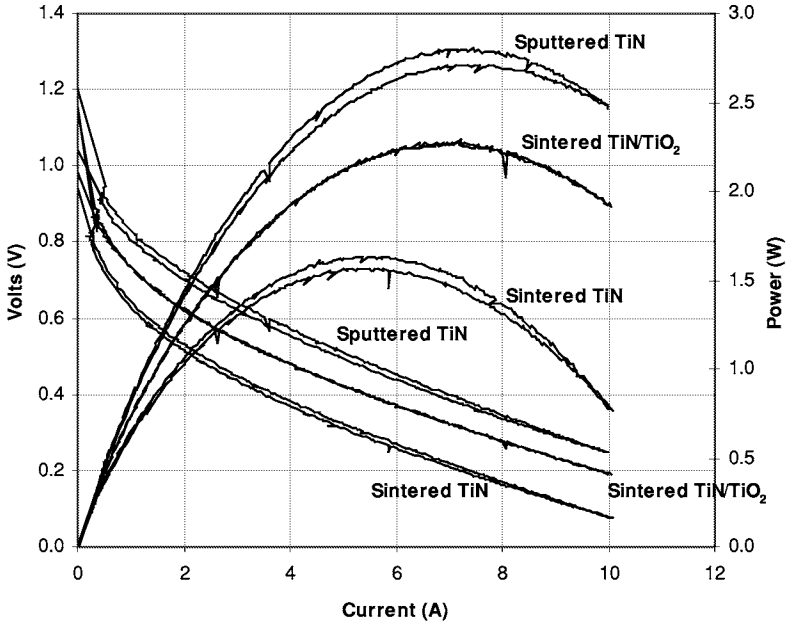

FIGURE 4. Comparison Plots of Sputtered TiN, Sintered TiN/TiO_2 and Sintered TiN Electrodes Evaluated in the Same METC at 850°C BASE Temperature. (I-V data correspond to the "Y" axis on the left of the chart. Power plots are computed from the I-V data and correspond to the "Y" axis on the right. Both the sintered and sputtered TiN electrodes exhibited power reductions on the return I-V sweep, whereas the sintered TiN/TiO_2 did not.)

Sintered TiN electrodes were fabricated with the same raw materials as those used in the MIECE electrodes of Figure 3b, but without the addition of TiO_2, and evaluated in an METC. The sintered TiN electrode was tested in situ with sputtered TiN and sintered TiN/TiO_2 electrodes in the same multi-electrode METC. A comparison of these I-V sweep test data and computed power values at 850°C BASE temperature are plotted in Figure 4. The two sintered electrodes were processed simultaneously; however, the sintered TiN/TiO_2 electrode exhibited a 39% increase in peak power over the sintered TiN electrode. The sintered TiN/TiO_2 electrode did not display the power reduction on the return I-V sweep, as did both of the electron conducting TiN electrodes. Using the data from Figures 3a and 3b, and after correcting for reduced BASE conductivity due to sodium vaporization cooling, it is

estimated on-average for the return sweeps of TiN/TiO_2 mixed conductor electrodes compared to the standard sputtered TiN electrode a system voltage improvement of ~ 18 mV with a corresponding resistive reduction ~ 20 mW/cm^2, and compared to the sintered TiN electrode a system voltage improvement of ~ 16 mV and a resistive reduction of ~ 10 mW/cm^2 were observed. The sputtered TiN electrode continued to outperform the sintered electrodes. The superior performance of the sputtered TiN electrode is attributed to its excellent uniformity and adhesion to the BASE surface. The authors believe that with optimized formulations, improved painted slurry application, and fully developed processing the sintered TiN/TiO_2 electrode could meet or exceed the performance of the sputtered TiN electrodes.

The exact mechanisms for how these MIECE behave are not known. Much work still remains in the understanding of how the combined sintered TiN/TiO_2 matrix transports sodium ions and the nature of its three-phase boundary (TPB). However, there are several aspects of ionic conductivity in TiO_2 that are reasonably well understood in the literature and permit a possible hypothesis as to what may be occurring in our electrodes. These formulations started with anatase TiO_2 powder, but anatase transforms to a permanent rutile structure at temperatures above 400°C; the exact temperature depends on a number of factors. Since all sintering temperatures exceed this transition range these electrodes were composed of TiN and TiO_2 rutile. The basic rutile lattice is illustrated in Figure 5 below. Open tunnel structures parallel to the "C" axis exist (Abrahams, et al., 1997), but do not exist in the "A" or "B" directions of the lattice. Figure 6 below shows views of these two aspects with titanium and oxygen atoms drawn to scale. Illustration "a" in Figure 6 shows a view of the "A-B" plane from the "C" direction. Parallel tunnels in the "C" direction are clearly seen and run the entire length of the crystal structure. Illustration "b" in Figure 13 is an "A" direction view of the "B-C" plane showing dense and fully blocked channels. Compounds with the rutile structure are often known to be intercalation compounds allowing ionic insertion into these tunnel structures. The larger tunnels are usually unstable without ions taking residence within them (McKinnon, 1997). These test data at high operational temperatures indicate stable and repeatable electrode performance. This observed stability suggests the presence of Na^+ ions within the TiO_2 matrix.

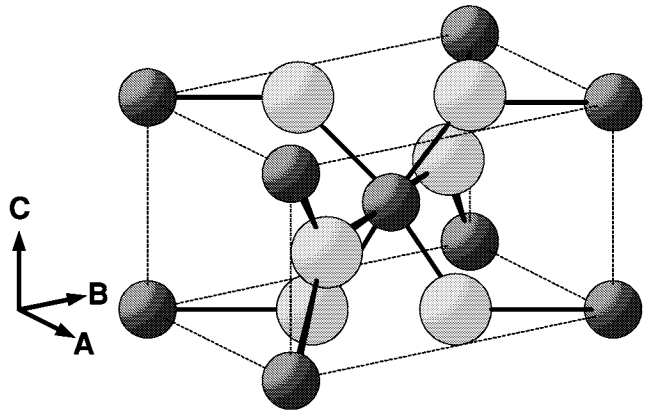

FIGURE 5. The Basic Crystal Lattice of TiO_2 Rutile Structure. (Titanium is represented as the darker spheres, while oxygen is represented as the lighter spheres. Note that the radii for each element are not to scale and are sized to permit their visual location within the lattice. Each oxygen atom has a coordination number of 3 titanium atoms, with Titanium having a coordination number of six oxygen atoms.)

TiO_2 could be formulated into sodium titanate and used as an AMTEC electrode because the sodium ions in such matrices are known to be loosely bonded in the matrix and used as a modest ionic conductor. Several sodium titanate compounds have been studied and found to readily display ion exchange, some at ambient temperatures (Nalbandyan, 1998). Nalbandyan also found that the stability of these structures increased with the increase of sodium in these structures. Holes of up to 4 Å have been noted in some sodium titanate structures at 410°C to 550°C when excited by an electron beam, thereby making room for multiple sodium ions in the tunnel (Bando, et al., 1980). Others have also noted the possibility of adding progressively more and more sodium ions to sodium titanates to improve their ionic and electronic conduction (Williams, 2001). A proposal has been made regarding the ion radius dimensions of Na^+ when in contact with the surface of rutile TiO_2 (San Miguel, et al., 2001). During *ab*

initio embedded cluster calculations, used for modeling the deposition of alkali atoms on the surface of rutile TiO_2, it was found that certain positional locations of sodium that are known to exist, could only occur if the radius of the surface adsorbed sodium ions were ~ 0.6 Å. It seems reasonable that such ionic radii are possible in the TiO_2 matrix, as well. If possible, then the ionic transport of sodium would be facilitated in the TiO_2 structure and in any sodium titanates formulated.

From these it is proposed that sodium ions leave the Na-BASE structure and are conducted into the TiN/TiO_2 electrode matrix. This activity augments the TPB, from just the surface of the Na-BASE to the available TPB sites throughout the structure of the porous TiN/TiO_2 electrode. The increased presence of Na in the electrode matrix at the higher current densities of the I-V sweeps permits this.

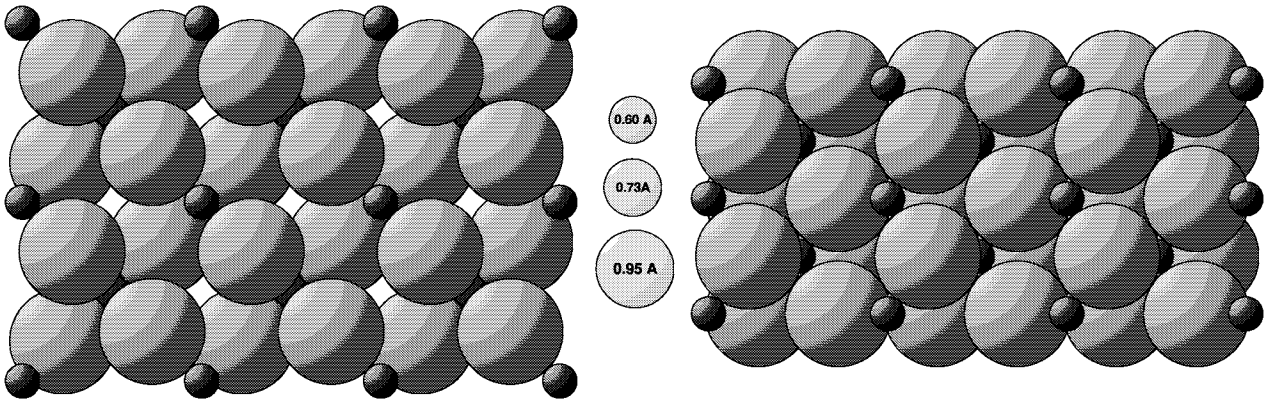

(a) The "A-B" plane rutile TiO_2 structure.

(b) The "C" plane rutile TiO_2 structure.

FIGURE 6. The TiO_2 Rutile Complex Structure as Seen Looking at the "A-B" Plane From the "C" Direction (illustration "a") and the "B-C" Plane Viewed From the "A" Direction (illustration "b"). (In these 'hard-sphere' representations the titanium and oxygen atoms are scaled to relative radii dimensions (Kingerly, et al., 1976). As in Figure 5 above titanium is represented as the darker spheres, while oxygen is represented as the lighter spheres. Note in illustration "a" that parallel channels in the "C" direction are clearly visible, while none are visible in illustration "b". The three vertically aligned spheres between the two structures represent sodium ions scaled to ionic radii of 0.60 Å, 0.73 Å and 0.95 Å.)

CONCLUSIONS

A mixed ionic and electronic conducting electrode (MIECE) for the Alkali Metal Thermal Electric Converter (AMTEC) made from TiN and TiO_2 has been proposed, made and tested. These test data suggest it behaves as a true MIECE due to its increased power response during the return leg of I-V sweeps with improvements in system voltage and reduced electrode resistance. This improved behavior is readily apparent in the power plots of the I-V sweep data for these electrodes as tested in miniature electrode test cell assemblies. Future work will involve more testing and material analysis to understand fully the mechanisms involved with these electrode formulations, and to determine the optimal mix ratios and processing conditions required to maximize the mixed conducting properties for this electrode.

ACKNOWLEDGMENTS

We wish to express our thanks to Tom Hunt, CEO of AMPS, for providing access to equipment, resources and invaluable guidance. We also want to thank Roger Williams and Amy Ryan, of the NASA Jet Propulsion Laboratory for their valuable suggestions and input regarding this work.

REFERENCES

Abrahams I., Bruce B. G., *Handbook of Solid State Electrochemistry*, P.J. Gellings and H.J.M Bouwmeester, editors; CRC Press, Boca Raton, 1997, p. 100.

Bando Y., Watanabe M., Sekikawa Y., "The Structure of Orthorombic, $Na_2Ti_9O_{19}$, a Unit-Cell Twinning of Monoclinic $Na_2Ti_9O_{19}$, Determined by 1-MV High-Resolution Electron Microscopy," *J. Solid State Chem.*, **33** p.413- 419 (1980).

Fletcher, R.W., Schwank, J.W., "Mixed Conductor Electrode Development for the Alkali Metal Thermal Electric Converter (AMTEC)," *Topical Conference Proceedings on "Fuel Cell Technology: Opportunities and Challenges"*, AIChE Spring, 2002, National Meeting, March 10-14, 2002, pp. 328-338.

Hunt T.K., C.A. Borkowski, K.F. Childs, R.K. Sievers, "Electrode Testing in Simple Vapor-Vapor AMTEC Cells," Proceedings *of the 32nd Intersociety Energy Conversion Engineering Conference*, 1997, p. 1196.

Kingerly W.D., Bowen H.K., Uhlmann D.R., *Introduction to Ceramics*, John Wiley Interscience Publications, New York, NY, 1976, p. 59.

McKinnon W.R., *Solid State Electrochemistry*, P.E. Bruce, editor; Cambridge Press, Cambridge, UK, 1997, p. 169.

Nalbandyan V.B., "Phase analysis and crystal chemical studies of sodium oxide – titanium oxide metal oxide systems," *Poster for 6th European Powder Diffraction Conference, Budapest, Hungary*, August 22-25, 1998, page 233 (1998).

Nowotny J., Radecke M., Rekas M., Sugihara S., Vance E. R., Weppner W., "Electronic and Ionic Conductivity of TiO2 Single Crystal Within the n-p Transition Range," *Ceram. Int.*, **24**, pp. 571-577 (1998).

Ryan M.A., Williams R.M., Lara L., Cortez R.H., Homer M.L., Shields V.B., "The Role of Titanium Dioxide in the Performance of Titanium Nitride AMTEC Electrodes," #399, *196th Meeting of the Electrochemical Society,* 1999.

Ryan M.A., Williams R.M., Lara L., Fiebig B.G., Cortez R.H., Kisor A.K., Shields V.B., Homer M.L., "Advances in Electrode Materials for AMTEC," in proceedings of *Space Technology and Applications International Forum (STAIF-2001)*, edited by M.S. El-Genk, AIP Conference Proceedings 552, 2001, pp.1008-1093.

San Miguel M.A., Calzado C.J., Sanz J.F., "Modeling Alkali Atoms Deposition on TiO_2 (110) Surface," *J. Phys. Chem. B*, **105**, 1794-1798 (2001).

Williams R. M., personal correspondence to Tom Hunt, March 2, 2001.